land

Article

Runoff and Evapotranspiration–Precipitation Ratios as Indicators of Water Regulation Ecosystem Services in Urban Forests

Urša Vilhar

Department of Forest Ecology, Slovenian Forestry Institute, Večna pot 2, SI-1000 Ljubljana, Slovenia; ursa.vilhar@gozdis.si; Tel.: +386-(0)1-200-78-46

Abstract: As a form of green infrastructure, urban forests play a key role in the provision of hydrological ecosystem services (ESs) in cities. Understanding how urban forest structure and soil properties influence water regulation ESs is crucial for managing and planning green infrastructure in cities. We analysed two indicators—the runoff to precipitation (Q/P) and the evapotranspiration to precipitation (ETP/P) ratios—for five different urban forests. We used the hydrological model Brook90 over 16 years to simulate runoff, evapotranspiration, canopy interception, transpiration and soil evaporation. The results showed that mixed forests have the highest water retention capacity, with the lowest Q/P (0.41) and the highest ETP/P (0.59). In contrast, riparian deciduous forests had the lowest water retention capacity, with the highest Q/P (0.75) and the lowest ETP/P (0.25). Both indicators showed similar annual and seasonal results. However, Q/P showed strong inter-annual variation and a strong correlation with precipitation, while ETP/P remained consistent despite precipitation fluctuations in the observed years. In conclusion, the ETP/P ratio is better suited to assess the water regulation ES of urban forests.

Keywords: stand structure; tree species composition; soil properties; hydrological model Brook90; urban ecosystems; precipitation; transpiration; urban green space; urban green infrastructure

Academic Editors: Alessio Russo and Giuseppe T. Cirella

Received: 21 February 2025
Revised: 23 March 2025
Accepted: 31 March 2025
Published: 9 April 2025

Citation: Vilhar, U. Runoff and Evapotranspiration–Precipitation Ratios as Indicators of Water Regulation Ecosystem Services in Urban Forests. *Land* **2025**, *14*, 809. https://doi.org/10.3390/land14040809

1. Introduction

Ecosystem services (ESs) are generally defined as the benefits that humans derive from ecosystems [1–3]. They are a powerful framework for understanding human relationships with the environment and shaping environmental policy [4] and are generally categorised into provisioning, regulating, supporting and cultural services [5]. Among the myriad services provided by ecosystems, hydrological services such as water purification and water supply are considered key to the realisation of other ecological services such as drinking water, recreation and human health [4,6]. Water regulation, which is considered one of the most important regulating ES in ecosystem accounting, includes several ES, such as water retention and protection from storms and floods (including flood defence in rivers and along coasts) [7]. These water regulation services are closely related to other regulating ES, such as erosion and sedimentation control and water purification. Unfortunately, hydrological ecosystem services are under serious threat and are rapidly declining in many watersheds around the world [8]. The availability and supply of freshwater is becoming increasingly unreliable due to increasing climate variability and change, air, soil and water pollution, groundwater depletion, sea level rise and shrinking snowpacks and glaciers [9]. Linking hydrological processes (e.g., energy and water cycles) to ecosystem services (e.g., carbon sequestration, water quality improvement, biodiversity conservation, regulation of water and nutrient cycles, mitigation of the urban heat island) [8] is crucial for an adequate quantification of ecosystem functions [10] and services [4]. This is particularly important for projecting future responses of urban areas to climate change and variability [11], land-use change [12], natural resource management options [13] and human disturbances (e.g., urbanisation) [14,15]. As the importance of ES is increasingly recognised, there is also a growing need for tools and models that can provide decision-makers with information on the provision of services and the impacts of natural resource management on these services [16].

Urban forests as a form of "green infrastructure" are one of the main providers of ES in urban areas [17,18]. The most recognised benefits resulting from their hydrological role are stormwater runoff reduction [19], stormwater retention, flood regulation [20] and water quality protection [21]. Previous studies have shown that urban forests play an important role in the hydrology of urban areas by intercepting precipitation, which reduces throughfall and thus peak flows in the catchment [22]. Through the process of transpiration, water stored in the soil moves through the tree into the atmosphere [23], increasing the availability of pore space in the soil for future storm events. However, overall tree transpiration rates and water use and their effects on runoff can vary greatly and depend on the structure of urban forests, including tree species composition, geometry of the canopy, tree size and leaf area [24–26] as well as management context and climate factors [27].

The majority of research on water regulation in forests comes from studies conducted in rural forests or individual street and park trees in urban environments [27–29], although hydrological fluxes vary greatly depending on climate, geography and ecosystem type. In urban areas, for example, urbanisation has been shown to impact meteorological and hydrological dynamics equally. The artificial thermal properties and increased particle pollution in urban areas influence the way precipitation is generated. The enhanced wind-driven precipitation can promote the development of convective summer thunderstorms [30,31]. The expansion of urban areas leads to an increase in impervious surfaces and the expansion of artificial drainage networks, which can facilitate dramatic changes in the magnitude, pathways and timing of runoff at different scales [32], from individual buildings to larger urban agglomerations [33,34]. For this reason, researchers are increasingly attempting to assess the water regulation capacity of urban forests in addition to studying individual urban trees [35] or rural forests [36]. The lack of empirical studies in cities [18] points to the need for an empirical method to derive runoff and evapotranspiration rates in order to fully determine the urban water balance [33]. Furthermore, the quantification of evapotranspiration fluxes is increasingly being introduced as a sustainable technique to manage stormwater runoff in urban areas [37].

The existing literature shows a gap in scientific understanding and empirical evidence regarding the relationships between urban forest structure, soil properties and water regulation ES. This is crucial for the development of ES-based management tools for urban watersheds [38] to maintain water regulation ES. In addition, the characteristics of urban forests that may influence hydrological fluxes are difficult to identify, as these ecosystems are highly heterogeneous and, to a large extent, (un)managed by private forest owners with different (or lack of) management preferences [39]. Furthermore, there is little information on how water regulation ES in urban forests are affected after canopy release and the establishment of natural forest regeneration.

To address this gap, the study aims to analyse how urban forest structure (e.g., geometry of the canopy and understorey, species composition and age structure of forest stands) affects water regulation ES in the city of Ljubljana. In particular, the water regulation capacity of the vegetation and soil in the canopy gaps was compared with that of nearby urban forests by comparing different components of the hydrological cycle, e.g., precipitation (P), runoff (Q) and ecosystem evapotranspiration (ETP). For this purpose, the hydrological model Brook90 was used to simulate the hydrological fluxes in the gaps and forests over a 16-year period. In addition, two indicators were selected to assess the water regulation ES of urban forests and their applicability was tested: the runoff to precipitation ratio (Q/P) and the evapotranspiration to precipitation ratio (ETP/P). The values of the Q/P and ETP/P ratios were compared between urban forests on an annual and seasonal basis. It is hypothesised that urban forests with the lowest Q estimates and the highest ETP/P values have a higher water regulation capacity. Furthermore, the applicability of these two indicators was tested and their potential applications discussed. Specifically, we compare the data requirements, ease of use and interpretability of results between the indices to help decision makers in their search for an easy-to-use indicator of urban forest water regulation ES.

The results of this study could have a positive impact on hydrologically oriented urban forest management measures [40], optimised urban water resource management [38] and the planning of urban green infrastructure [41]. Moreover, this study has the urgency to promote urban forests as one of the urban natural water retention measures (NWRM) [42,43] and nature-based solutions (NBS) not only for providing services to mitigate the impacts of natural water-related hazards, but also for their contribution to climate change mitigation and biodiversity in cities. Despite the many benefits of NBS, its implementation has so far been rather limited [44].

2. Materials and Methods

2.1. Site and Stand Description

The urban forests studied are located in the city of Ljubljana, Slovenia (46°04′ N, 14°31′ E) with a population of 280,140 inhabitants [45]. The Slovenian capital is located in the Ljubljana Basin, which is characterised by a continental climate (CfB according to the Köppen climate classification system) with clearly defined seasons. The average annual precipitation is 1393 mm and the average annual air temperature is 9.8 °C. The interannual variability of precipitation is quite high, with maximum precipitation in summer and autumn [46]. The urban forest sites were established in a transect from an urban mixed forest (upland forest) and a gap in the city centre to a riparian pine forest, a deciduous forest and natural regeneration on a small island in the Sava River. The stand characteristics (Table 1) and soil properties of the urban forests (Table 2) were recorded according to the ICP Forests protocols [47,48].

Table 1. General characteristics of the urban forest plots in the city of Ljubljana, Slovenia.

Urban Forest Site	Plot	Slope (%)	Aspect	Tree Height (m)	Stem Volume (m^3 ha^{-1})	Canopy Cover (%)	Ground Vegetation Cover (%)
Riparian forest	Pine forest	2 *	south-east *	11.7 *	151.1 *	50 *	100 *
	Deciduous forest	2 *	south-east *	15.8 *	246.9 *	30–50 *	80–100 *
	Regeneration	1 *	/	17.5 *	/	80–100 *	/
Mixed (upland) forest	Forest	3 **	south-east **	21.9 **	589.1 **	90–100 **	/
	Canopy gap	3 **	south-east **	/	/	/	100 **

* [49]; ** [50].

Table 2. Soil properties of the urban forests in the city of Ljubljana, Slovenia.

Urban Forest Site	Plot	Soil Type (WRB, 2007)	Soil Depth ** (cm)	Stoniness ** (% vol)	Soil Organic Matter ** (%)	Soil Texture Class **	Bulk Density ** (g cm^{-3})	Field Capacity ** (−33 kPa) (m^3 m^{-3})	Permanent Wilting Point ** (−1500 kPa) (m^3 m^{-3})
Riparian forest Gameljne	Pine forest	Fluvisols *	0–5	39.9	7.2	Sandy loam	1.0	0.2	0.1
			5–10	28.0	4.3	Sandy loam	1.1	0.2	0.1
			10–15	2.1	2.6	Sandy loam	1.6	0.2	0.0
	Deciduous forest	Fluvisols *	0–5	0.0	8.6	Silty loam	0.7	0.4	0.2
			5–10	0.0	3.9	Silty loam	0.9	0.4	0.1
			10–20	0.0	2.2	Silty loam	1.1	0.4	0.1
			20–40	0.1	1.5	Silty loam	1.1	0.3	0.1
			40–60	8.6	0.9	Sandy loam	1.3	0.3	0.0
			60–80	28.1	0.8	Sandy loam	1.6	0.1	0.0
	Regeneration	Fluvisols *	0–5	44.7	4.3	Loamy sand	1.1	0.3	0.1
			5–10	7.7	1.0	Loamy sand	1.0	0.3	0.1
			10–20	42.2	0.9	Sandy loam	1.0	0.2	0.1
			20–40	3.3	0.8	Sandy loam	1.5	0.1	/
			40–50	4.6	0.9	Sandy loam	1.3	0.2	0.1
Mixed forest Rožnik	Forest and Canopy gap	Dystric cambisols **	0–5	11.0	7.7	Silty clay loam	0.6	0.5	0.1
			5–10	16.6	3.7	Silty loam	0.8	0.4	0.1
			10–20	22.8	2.6	Silty clay loam	1.0	0.4	0.2
			20–40	17.2	1.5	Silty clay loam	0.9	0.3	0.2
			40–60	18.4	0.8	Silty clay loam	1.1	0.3	0.2
			60–80	22.1	0.5	Silty clay loam	1.3	0.4	0.2

* [49]; ** [50].

2.1.1. The Mixed Forest

The upland "mixed forest" and the "canopy gap" plots are located in the Tivoli, Rožnik and Šišenski Hrib Landscape Park in the centre of the city of Ljubljana (Figure 1).

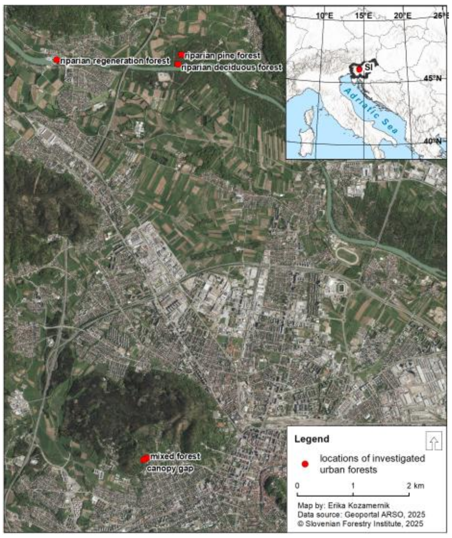

Figure 1. Locations of investigated urban forests within the city of Ljubljana: the mixed forest; the canopy gap in the mixed forest; the riparian pine forest; the riparian deciduous forest, and the riparian regeneration.

Since 2010, most of the forest area has been protected due to its highly valued social and ecological forest ecosystem services [50]. The site is 310 m above sea level and the forest canopy consists of sessile oak (*Quercus petraea* (Mattuschka) Liebl.), sweet chestnut (*Castanea sativa* (Mill.)) and spruce (*Picea abies* (L.) Karst.). The forest floor vegetation contains only a few species in the shrub and herb layer. The mixed forest consists of a 0.25 ha (50 × 50 m) plot. The canopy is very dense. The gap in the canopy was created in 2014 after an ice storm and bark beetle logging and consists of a 0.01 ha (10 × 10 m) plot. The subsoil consists of sedimentary rock (shale, clay and quartz sandstone). The soil was classified as Dystric Cambisol [51]. The thickness of the O horizon was 0 to 6 cm, and the depth of the M horizon was between 0 and 130 cm, with a Silty clay loam texture [50].

2.1.2. The Riparian Forest

(a) The Pine Forest

The 0.25 ha (50 × 50 m) pine forest plot is located on an elevated river terrace, outside the direct influence of the Sava River. The plot is 300 m above sea level, and the canopy consists of Scots pine (*Pinus sylvestris* L.) in the upper canopy layer (78% of total growing stock) and a mixture of deciduous tree species in the middle and lower canopy layer, such as small-leaved lime (*Tilia cordata* Mill.), sessile oak (*Quercus petraea* (Mattuschka) Liebl.) and hornbeam (*Carpinus betulus* L.). The canopy is very loose (fragmented) and contains fairly dense shrub and forest floor vegetation [49]. The subsoil consists of glacial-fluvial gravel, and the soil has been classified as Fluvisols (WRB 2007). The thickness of the O horizon was 0 to 6 cm and the depth of the M horizon was 0 to 40 cm, with a sandy-loam texture [50].

(b) The Deciduous Forest

The 0.25 ha (50 × 50 m) deciduous forest plot in the floodplain is about 2 m above the terrace of the Sava River during the daily high water at 296 m above sea level [49]. The forest canopy consists of sycamore maple (*Acer pseudoplatanus* L.), grey alder (*Alnus incana* (L.)

Moench.), small-leaved lime (*Tilia cordata* Mill.), European ash (*Fraxinus excelsior* L.), willow (*Salix* sp.), black poplar (*Populus nigra* L.), etc. The canopy is loose, and the vegetation on the forest floor is quite dense. This plot is particularly prone to frequent flooding. The subsoil consists of glacial fluvial gravels, and the soil has been classified as Fluvisols (WRB 2007). The thickness of the O horizon was 0 to 4 cm, and the depth of the M horizon was between 0 and 90 cm, with a clay-loam texture [50].

(c) The Forest Regeneration

The forest regeneration plot (0.30 ha) is located on a small island in the Sava River at an altitude of 302 m above sea level. The natural forest regeneration of the deciduous forest on the river bank is in the pole saplings stage, is not managed and is left to develop naturally. The tree layer is dense and consists mainly of black poplar (*Populus nigra* L.), willow (*Salix* sp.) and European ash (*Fraxinus excelsior* L.). This site is also frequently flooded [49]. The subsoil consists of glacial fluvial gravels, and the soil has been classified as Fluvisols (WRB 2007). The thickness of the O horizon was 0 to 2 cm, and the depth of the M horizon was between 0 and 50 cm, with a clayey sand texture [50].

2.2. Indicators of Water Regulation Ecosystem Services (ES)

Water regulation ES refer to the regulation of hydrological fluxes [52,53] and is derived from the relationships between input (precipitation, P) and output (runoff, Q). To quantify the water regulation ES, we considered using the approach of conceptual methods to estimate the water balance to divide the hydrological cycle into different components [54], e.g., precipitation (P), runoff (Q) and evapotranspiration (ETP), which consists of I, TRAN and SE and is often referred to as ecosystem evapotranspiration [55]:

$$P = Q - ETP, \tag{1}$$

$$ETP = I - TRAN - SE \pm \Delta SMC, \tag{2}$$

where P is precipitation in the open; Q refers to all forms of drainage or runoff, e.g., unsaturated flow and saturated flow through the soil matrix and macropores; ETP is actual evapotranspiration and consists of I, TRAN and SE. I is evaporation from moist canopy surfaces, such as intercepted water; TRAN is transpiration from the canopy and understory vegetation; and SE is evaporation from the soil or soil evaporation (SE). ΔSMC is the variation in soil moisture content, which is assumed to be 0 in the long term.

These components of the hydrological cycle were measured (P and SMC) or simulated (ETP, I, TRAN, SE) for each urban forest using the Brook90 water balance model [56] over a 16-year period from 2007 to 2022.

In addition, two indicators of water regulation ES were assessed and their applicability to urban forests tested: (a) the runoff to precipitation ratio (Q/P) and (b) the evapotranspiration to precipitation ratio (ETP/P), also referred to as evaporation ratio [57] or evaporative index [58,59]. The ETP/P is defined as the ratio between the evaporation that actually occurs in a given area under natural conditions and the precipitation that falls on that area [57]. It should be emphasised that none of the statements made here refer to theoretical estimates of potential reference crop evapotranspiration (PET) [60], but to actual evapotranspiration (ETP), which is determined by the many factors that affect soil and plant moisture and cause some moisture to escape into the atmosphere.

2.3. Meteorological Data and Soil Hydrological Measurements

Meteorological monitoring in urban forests was carried out as part of the Intensive Monitoring of Forest Ecosystems [61] in accordance with the harmonised guidelines of the International Cooperative Programme on Assessment and Monitoring of Air Pollution

Effects on Forests (ICP Forests), the United Nations Economic Commission for Europe Convention on Long-range Transboundary Air Pollution [62] and the Life+ EMoNFUr project [50]. The hourly mean values of air temperature and humidity, wind direction and speed, global radiation and hourly precipitation totals were recorded with automatic weather stations (Davis instruments, Hayward, CA, USA) in open areas according to ICP Forests [63] at a distance of less than 1 km from the forest site [64]. Missing data on air temperature, humidity and global radiation were replaced by data from the Ljubljana meteorological station (archive of the Slovenian Environment Agency) using site-specific regression functions [64].

Precipitation and throughfall were monitored from 1 March 2007 to 31 December 2022 in the plots in the mixed forest and from 1 March 2007 to 31 December 2019 in the plots in the riparian forest. The samples were taken manually every fortnight in the mixed forest plots and monthly in the riparian forest plots. The mixed forest plot was equipped with eight systematically distributed, fixed funnel samplers (0.23 m diameter), which were placed 140 cm above the ground. In addition, the throughfall was collected with ten systematically distributed gutter samplers (3 m long pipe, 4 cm diameter, with three 87 cm long and 0.9 cm wide slots in rows), the upper part of which was placed 0.60 m above the forest floor and drained directly into polythene containers that served as sumps [25]. The total sampling area on the 0.25 ha plot was 0.52 m^2 (the collection area of each funnel collector was 415 cm^2 and of each gutter 185 cm^2). From 2007 to 2012, the riparian pine forest and deciduous forest were equipped with three randomly placed funnel samplers (0.24 m diameter) installed 130 cm above the ground [25]. The total sampling area on the 0.25 ha plot was 0.14 m^2 (the sampling area of each funnel sampler was 452 cm^2). In winter 2012, ten funnel samplers (0.16 m diameter) and three snow samplers (0.23 m diameter) were installed 140 cm above the ground and distributed using a combination of systematic and randomised approaches, as recommended by Clarke et al. [65]. The total sampling area on the 0.25 ha plot was 0.20 m^2 (the sampling area of each funnel sampler was 201 cm^2). Precipitation was measured in a neighbouring meadow (an open area), approximately 100 m outside each forest. Three fixed precipitation samplers (0.23 m diameter) in the growing season and three snow samplers (0.23 m diameter) in winter were installed 140 cm above the ground [65], as precipitation in a solid state requires different collection methods [66]. The amounts of incident precipitation and throughfall were measured in the field using a measuring cylinder.

The precipitation data were combined to coincide with the sampling periods for throughfall and were gap-filled using a linear regression between the measured incident precipitation in the urban mixed and riparian forests and the precipitation at the Ljubljana meteorological station (299 m above sea level; 46°04′ N, 14°31′ E) (Archive of the Slovenian Environment Agency) [25,64,67]. Missing data on throughfall in the mixed forest were gap-filled using linear regression between funnel and gutter collectors. Missing data on throughfall in riparian pine forest, deciduous forest and regeneration were gap-filled using a linear regression between measured precipitation and throughfall on urban forest plots [67].

The potential reference crop evapotranspiration (PET) is defined as the amount of water that evaporates from the reference plant and the soil. The standard reference area is an actively growing grass that completely covers the soil and is sufficiently supplied with water, has a height of 0.12 m, a surface resistance of 70 s m^{-1} and an albedo of 0.23. The daily PET values were calculated at the Ljubljana meteorological station from 2007 to 2022 (archive of the Slovenian Environment Agency) using the Penman-Monteith method [60] and aggregated to annual, monthly and seasonal values.

Using representative soil samples from the predominant soil units, the available water capacity of the mineral soil horizons for each urban forest was calculated as the difference between the pressure plate measurements of field capacity (soil moisture content at 0.033 MPa) and the permanent wilting point (soil moisture content at 1.5 MPa) [50]. The soil moisture content of the 0 to 40 cm thick soil layer was measured monthly at three locations on each plot in the riparian forest using Time Domain Reflectometry (TDR, Prenart Equipment, Frederiksberg, Denmark). The dual probes were installed vertically and passed through the 40 cm soil layer, including the organic layer. Soil-specific calibration curves for vertical TDR probes were used, which were determined using the calibration procedures described in Dirksen [68]. In the mixed forest, three automatic soil moisture sensors (TEROS-10, METER Group, Inc., Pullman, WA, USA) were installed in each plot at 15 cm, 50 cm and 75 cm soil depth, which measured soil moisture content at 30 min intervals and aggregated to daily values.

2.4. The Brook90 Hydrological Model

The Brook90 model was chosen because it has been shown in previous studies to be suitable for simulating the hydrological fluxes of tall forests and canopy gaps in highly structured forest ecosystems and heterogeneous forest soils with low water storage capacity [69–72]. The model has more than 100 physically based input parameters, which are generally simple and easy to adjust [70]. Several parameterisation options for forest stands allow the model to describe the complexity of the horizontal and vertical structure of forest stands and soil properties more comprehensively [69]. The model calculates daily water fluxes (tree transpiration, canopy interception, throughfall, stemflow, soil evaporation, snow evaporation, drainage (or runoff)) and soil moisture content at different depths or for the entire root depth. Tree transpiration and soil evaporation are calculated separately using the Shuttleworth-Wallace method [73], which has been modified to separate daytime evaporation from nighttime evaporation [56]. An important feature of the Brook90 model is that it only considers homogeneous plant cover at a selected site or catchment. Therefore, the differentiation between forests, canopy gaps and regeneration was achieved by measured or preset input parameters corresponding to different forest development stages, plant height and density, leaf area index, interception and other ecophysiological characteristics, such as macropore or bypass flow [69,72]. Further information on model parameterisation can be found in [56,69,70,74].

2.5. Model Fitting and Testing

Site-specific parameters for running the Brook90 model were derived by fitting the model output with measured throughfall data from 2007–2014 and testing it with throughfall data from 2015–2019 for riparian forests and from 2015 to 2022 for mixed forests. An additional model fit was performed for each plot by comparing simulated and measured soil moisture data with the datasets for 2007–2008 for the riparian forests and from 16 November 2021 to 30 June 2022 for the mixed forests. An additional model test was performed with the measured soil moisture datasets 2009–2012 for the riparian forests and from 1 July 2022 to 31 December 2022 for the mixed forests.

The goodness of fit was assessed using the linear correlation coefficient (r), which describes the degree of agreement between measured and simulated values, the index of agreement (D) [75], which is a descriptive measure of the relative error, and the root mean square error (RMSE), which expresses the error between the measured and simulated values [67].

2.6. Data Analysis and Statistical Methods

Microsoft Excel was used to review and process the data. GraphPad Prism® version 10.4.0 (621) for Windows [76] was used to perform the statistical analysis.

The results of the entire study period were divided into two seasons for further investigation, according to the phenological development of the predominant tree species at each site (Archive of the Slovenian Environment Agency): a. Growing season, when deciduous trees fully develop their leaves (from 1 May to 31 October); b. Winter season, when deciduous trees have no leaves in their crowns (from 1 November to 30 April) [25]. This categorisation was made in particular because deciduous trees do not keep their leaves all year round, which significantly influences the variability of precipitation distribution [27,28,35,77]. In order to evaluate the influence of climatic conditions on the water regulation ES, the results for very wet and very dry growing seasons were also compared.

The Spearman correlation coefficient (ρ) was used to test the relationship between the simulated hydrological fluxes (Q, ETP, I, TRAN and SE) for five urban forests, and the coefficient of variation (CV) was used to measure the dispersion of the data from the average or mean value. The non-parametric Kruskal–Wallis test was used to test for differences in daily SMC and annual Q, ETP, I, TRAN and SE estimates between the five urban forests, with estimates matched to the simulation year. The Wilcoxon signed-rank test was used for post-hoc multiple comparison tests between the urban forests. The standard significance level (α) was set at 0.05.

3. Results

The weather data showed considerable interannual fluctuations from 2007 to 2022 (Figure S1). The annual P was lower than the long-term P (1981–2010) in 2007 (−12%), 2011 (−27%) and 2015 (−9%). In addition, the growing season PET/P ratio showed the highest water deficit in most years of the study period with values above the long-term annual mean (0.75), with maximum values in the growing season of 2009 (1.0), 2013 (0.91) and 2011 (0.91), followed by 2016 and 2017 (0.86). This corresponds to the multi-year drought period 2014–2018, as reported by several authors [78–80]. The mean annual air temperature was also highly variable compared to the long-term T (1981–2010). Only in 2010 was it lower (10.7 °C) than the long-term annual mean (10.9 °C). It was higher in all other years and reached its highest value in 2022 (12.9 °C), followed by 2014 (12.6 °C).

3.1. Model Fitting and Testing

Table S1 summarises the input parameters used in the Brook90 model simulations. Monthly throughfall (Figure S2) and daily soil moisture content (Figure S3) were well simulated for all forests both temporally and in magnitude. For the throughfall fitting, the average D value was 0.955 and the average RMSE was 19.7 mm month^{-1}. For the model testing, the average D value was 0.854 and the average RMSE was 20.45 mm month^{-1} (Table S2). For the soil moisture content fitting, the average D value was 0.803 and the average RMSE was 12.0 mm day^{-1}. For the model testing, the average D value was 0.806 and the average RMSE was 13.4 mm day^{-1} (Table S2).

3.2. Simulated Hydrological Fluxes

The soils in the mixed upland forests are classified as *Dystric Cambisols* [50] and can be up to 81 cm deep, while in the riparian forests much shallower *Fluvisols* are found [49], which are up to 50 cm deep and account for up to 34% of the stone volume (Table 2). The available water content measures the amount of water that the soil can retain for the plants through evapotranspiration and the amount that drains into the subsoil. It is achieved after gravity drainage of water from the macropores and typically occurs within

2–3 days after rainfall in uniformly structured, permeable soils. The highest available water capacity of mineral soils was measured for the mixed forest and canopy gap (126 mm), which corresponds to the highest soil depth of mineral soils (80 cm), followed by riparian deciduous forest (124 mm) with 50 cm mineral soil depth. The lowest available water capacity was measured for the riparian pine forest (33 mm), where the mineral soils were much shallower, reaching up to 20 cm depth.

Soil moisture content (SMC) data in the urban forests of our study were measured with different soil moisture sensors at different time periods. The agreement with the measured SMC was high in all urban forests (Figures S3 and S4, Table S2). To compare the SMC between all urban forests in our study in a harmonised approach, we compared the daily SMC values simulated with the hydrological Brook90 model for the period from 2007 to 2022.

In general, daily simulated SMC in riparian forests were much lower and showed less variability than in mixed upland forests and in the canopy gap (Figure 2). The highest average daily SMC in the growing season was simulated for the canopy gap (273 mm day^{-1}), followed by the mixed forest (164 mm day^{-1}). The lowest SMC was simulated for riparian regeneration (37 mm day^{-1}), followed by riparian pine forest (46 mm day^{-1}) and riparian deciduous forest (75 mm day^{-1}).

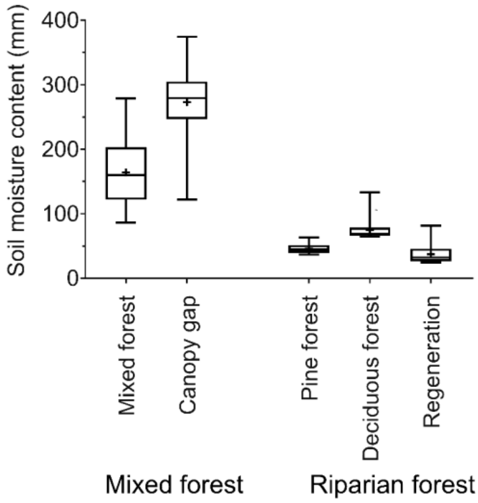

Figure 2. Box and Whiskers of daily growing season minimum, median and maximum soil moisture content (SMC) (mm day^{-1}), simulated by the hydrologic Brook90 model for urban forests from 2007 to 2022. "+" indicates mean.

Annual estimates of hydrological fluxes (Q, ETP, I, TRAN and SE) differed significantly between forests ($p < 0.001$). Annual Q estimates followed the pattern of annual P with the lowest values in 2011 and 2015, which were 73% and 81% of the average annual P from 2007 to 2022. Q estimates were higher for all forests in the relatively wet years 2010 and 2014, when annual P was more than 130% of the 2007–2022 mean.

In the mixed forest, annual Q estimates were lower (41% of P) and ETP estimates were higher (59% of P) compared to the other forests (Figure 3, Table 3). The same pattern was observed in winter, when Q estimates in the mixed forest were 53% of P and ETP 27% of P, and in the growing season, when estimated Q was 22% of P and ETP 76% of P. The winter ETP estimates in the mixed forest (27% of P) were similar to the annual ETP estimates of the riparian forests (25–27% of P).

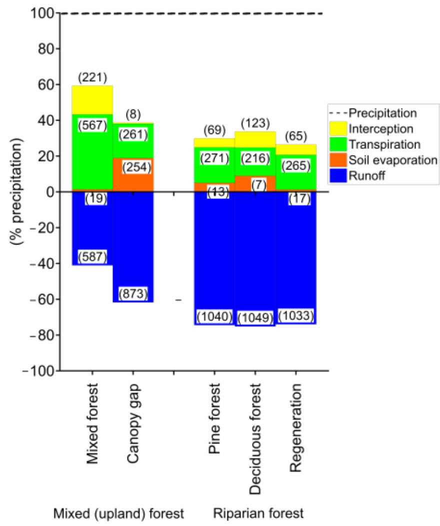

Figure 3. Mean annual canopy interception (I), transpiration (TRAN), soil evaporation (SE) and runoff (Q) as % of precipitation (P) for urban forests from 2007 to 2022. Figures in brackets are values in mm.

Table 3. Mean annual and seasonal runoff (Q), evapotranspiration (ETP) and its components: canopy interception (I), transpiration (TRAN) and soil evaporation (SE) as % of precipitation (P) for urban forests from 2007 to 2022.

		Mixed (Upland) Forest		Riparian Forest		
Years	**Hydrological Fluxes (% of P)**	**Forest**	**Canopy Gap**	**Pine Forest**	**Deciduous Forest**	**Regeneration**
2007–2022	Q	41	62	74	75	74
	SE	1	19	5	9	1
	TRAN	42	19	20	16	19
	I	16	1	5	9	6
	ETP = SE + TRAN + I	59	39	26	25	27
Growing season (2007–2022)	Q	22	41	61	64	61
	SE	2	27	2	1	2
	TRAN	56	28	28	19	26
	I	19	1	8	13	8
	ETP = SE + TRAN + I	76	56	38	33	36
Winter season (2007–2022)	Q	53	71	71	70	71
	SE	1	5	0	0	0
	TRAN	16	5	6	8	8
	I	9	0	1	3	2
	ETP = SE + TRAN + I	27	10	7	12	10

In the canopy gap, annual and seasonal Q estimates were higher and ETP estimates lower than in the mixed forest. In contrast, annual and growing season Q estimates were lower and ETP estimates higher in the canopy gap than in the riparian forests. However, winter Q estimates in the canopy gap were similar to those in riparian forests (71% of P), and ETP estimates were similar to those in riparian regeneration (10% of P).

Spearman correlation analysis showed that the annual Q estimates for each of the five forests under study were significantly correlated with each other ($R > 0.876$, $p < 0.001$), although the correlation was highest for riparian deciduous forest and riparian regeneration cases ($R = 0.994$, $p < 0.001$). For the annual ETP estimates, however, there was a statistically significant correlation for all forests ($R > 0.801$, $p < 0.001$), except the canopy gap ($p > 0.068$).

The difference between the estimated winter and growing season Q and ETP was largest in the mixed forest (31% of P for Q and 49% of P for ETP), followed by the canopy gap in the mixed forest (30% of P for Q and 46% of P for ETP). The smallest difference between the estimated seasonal Q and ETP was found for riparian deciduous forest (5% of P for Q and 21% of P for ETP), followed by riparian regeneration (10% of P for Q and 27% of P for ETP of P for Q).

As expected, the mixed forest had significantly higher annual TRAN estimates (TRAN = 42% of P) compared to the other forests ($p < 0.001$). Annual TRAN estimates were significantly lower in riparian deciduous forest (16% of P), but similar in mixed forest canopy gap (19%), riparian regeneration (19%) and riparian pine forest (20%). Annual TRAN estimates were highly correlated in the case of riparian deciduous forest and regeneration (R = 0.959, $p < 0.001$). The lowest correlation of TRAN estimates was found for mixed forest and canopy gap (R = 0.643, $p = 0.007$). The difference between the estimated seasonal TRAN was largest in the mixed forest (40% of P), followed by the canopy gap (24% of P) and the riparian pine forest (22% of P). The smallest difference between estimated seasonal TRAN was in riparian deciduous forest (11% of P), followed by riparian regeneration (19% of P).

Annual SE estimates were significantly higher ($p < 0.001$) in the canopy gap (19% of P) compared to the other plots, followed by riparian deciduous forest (9% of P). The lowest annual SE estimates were in mixed forest and riparian regeneration (1% of P), followed by riparian pine forest (5%). Statistical tests showed that annual SE estimates were significantly correlated in the case of mixed forest and riparian pine forest (R = 0.826, $p < 0.001$), followed by riparian deciduous forest (R = 0.786, $p < 0.001$), and the regeneration (R = 0.735, $p = 0.001$). There was no statistically significant correlation between the estimated annual SE for the canopy gap and other plots ($p > 0.066$). The difference between the estimated seasonal SE was largest in the canopy gap (22% of P) and was less than 1.7% of P in all other plots.

Annual I estimates differed significantly among the five forests ($p < 0.001$) and were lowest in the canopy gap (<1% of P), followed by the riparian pine forest (5%), riparian regeneration (6%), and deciduous forest (9%). Annual I estimates were highly correlated in the case of mixed forest and riparian deciduous forest (R = 0.955, $p < 0.001$), followed by riparian pine forest (R = 0.907, $p < 0.001$) and regeneration (R = 0.928, $p < 0.001$). There was no statistically significant correlation between the estimated annual I for the canopy gap and other forests ($p > 0.183$). The difference between the estimated seasonal I values was highest in riparian deciduous forest (10% of P), followed by mixed forest (9% of P) and riparian pine forest (8% of P). The smallest difference between the estimated seasonal I values was in the canopy gap (1% of P).

3.3. Indicators of Water Regulation Ecosystem Services (ES)

The lowest water retention capacity was found in riparian deciduous forest, where the mean annual Q/P was highest (0.75) and the ETP/P was lowest (0.25) (Figure 4, Table 4). This was followed by the riparian pine forest, where the mean annual Q/P was 0.75 and the ETP/P was 0.26. Both indicators showed the highest water retention capacity in the mixed forest, where the mean annual Q/P ratio was the lowest (0.41) and ETP/P the highest (0.59). In the growing season, Q/P in the mixed forest was only 0.21 and ETP/P 0.77, while in the winter season Q/P was 0.69 and ETP/P 0.39. A similar pattern was observed in the growing season, where both indicators showed the highest water retention capacity in the mixed forest with the lowest Q/P (0.21) and highest ETP/P ratio (0.77). In the growing season, the lowest water retention capacity was observed in the riparian deciduous forest, where the seasonal Q/P ratio was the highest (0.63) and the ETP/P ratio the lowest (0.33). In contrast, during winter, both indicators showed the lowest water retention capacity in the riparian pine forest, where the seasonal Q/P ratio was highest (0.92) and the ETP/P ratio lowest (0.11). The highest water retention capacity in winter was found for the mixed forest with the lowest Q/P (0.69) and the highest ETP/P ratio (0.39). The difference between the seasonal Q/P and ETP/P ratios in the winter and growing season was greatest in the canopy gap (0.51 for Q/P and 0.42 for the ETP/P ratio), followed by the mixed forest (0.48 for Q/P and 0.38 for the ETP/P ratio). In contrast, the seasonal Q/P and ETP/P differences were smallest in the riparian deciduous forest (0.28 for Q/P and 0.18 for the ETP/P ratio).

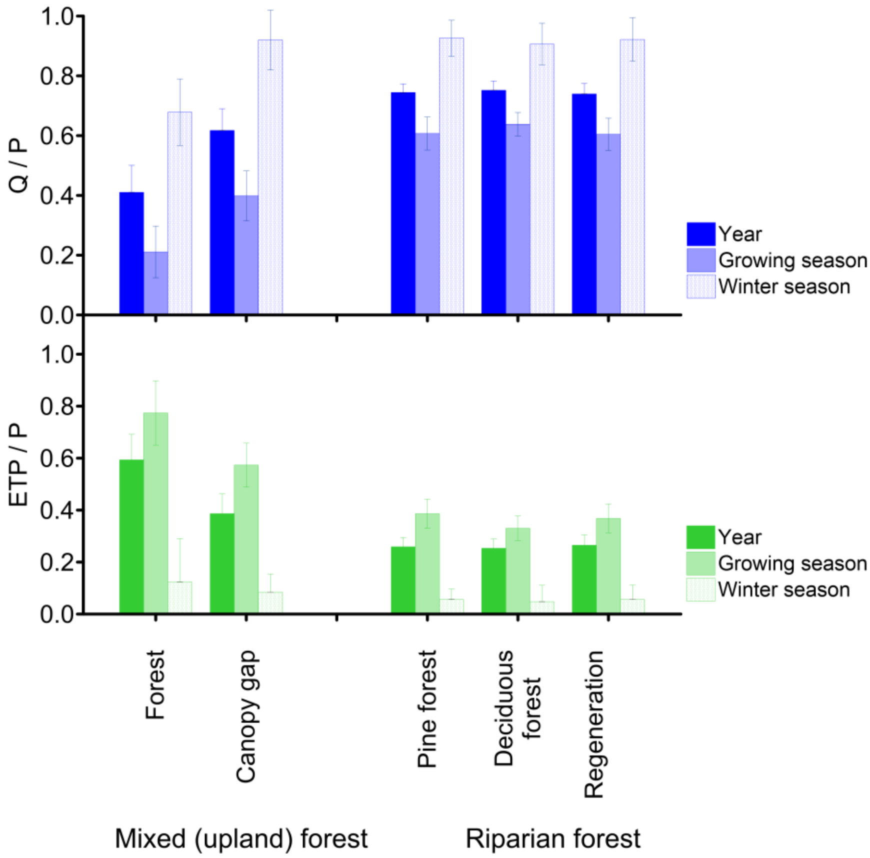

Figure 4. Mean annual and seasonal runoff–precipitation (Q/P), and evapotranspiration–precipitation (ETP/P) ratios for urban forests from 2007 to 2022.

Table 4. Mean annual and seasonal runoff–precipitation (Q/P), and evapotranspiration–precipitation (ETP/P) ratios for urban forests from 2007 to 2022.

		Mixed (Upland) Forest						Riparian Forest								
Years	**Ratio**	**Forest**			**Canopy Gap**			**Pine Forest**			**Deciduous Forest**			**Regeneration**		
		Mean	**Min**	**Max**	**Mean**	**Min**	**Max**	**Mean**	**Min**	**Max**	**Mean**	**Min**	**Max**	**Mean**	**Min**	**Max**
2007–2022	Q/P	0.41	0.26	0.57	0.62	0.46	0.75	0.75	0.71	0.79	0.75	0.69	0.81	0.74	0.67	0.80
	ETP/P	0.59	0.43	0.77	0.39	0.25	0.55	0.26	0.19	0.32	0.25	0.20	0.32	0.26	0.20	0.34
Growing season (2007–2022)	Q/P	0.21	0.10	0.40	0.40	0.20	0.60	0.60	0.50	0.70	0.63	0.60	0.70	0.60	0.50	0.70
	ETP/P	0.77	0.60	1.00	0.58	0.40	0.70	0.39	0.30	0.50	0.33	0.20	0.40	0.36	0.20	0.50
Winter season (2007–2022)	Q/P	0.69	0.50	0.90	0.91	0.80	1.20	0.92	0.80	1.10	0.91	0.80	1.10	0.91	0.80	1.10
	ETP/P	0.39	0.20	0.70	0.16	0.10	0.30	0.11	0.10	0.20	0.16	0.10	0.30	0.13	0.10	0.30

In order to thoroughly consider the impact of climatic conditions on water regulation ES, we analysed seasonal variations of Q/P and ETP/P ratios (Figure 5). The lowest amount of precipitation was observed in the 2009 growing season (632 mm) and the highest in the 2010 growing season (1044 mm) in the observation period (average growing season P = 785 mm). Growing season Q/P ratios reached the lowest values in the year 2009 in mixed forest (0.12), riparian pine forest (0.51) and riparian regeneration (0.53). In the canopy gap, the lowest growing season Q/P was in the year 2011 (0.25), and in the riparian deciduous forest, it was in the year 2016 (0.59). Growing season Q/P ratios were highest in year 2022 in mixed forest (0.39), riparian pine forest (0.70), deciduous forest (0.73) and riparian regeneration (0.72). In the canopy gap, the highest growing season Q/P was in the year 2012 (0.44). Growing season ETP/P ratios reached the lowest values in the year 2009 in all urban forests, ranging from 0.40 in riparian deciduous forest to 1.05 in mixed forest. The highest growing season ETP/P ratios were in the year 2010 in the canopy gap (0.37) and riparian pine forest (0.28), whereas in other urban forests, the highest growing season ETP/P ratios were in the year 2022.

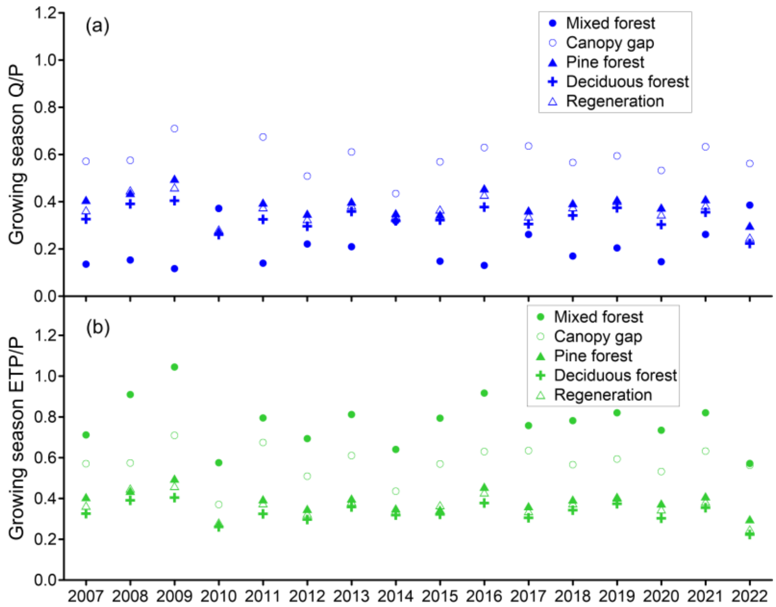

Figure 5. (**a**) Growing season runoff–precipitation ratio (Q/P) and (**b**) Growing season evapotranspiration–precipitation ratio (ETP/P) for urban forests from 2007 to 2022.

The two proposed indicators of water regulation ES, the Q/P and ETP/P ratios, showed similar results for selected urban forests on the annual and seasonal time scales. However, when comparing the interannual Q/P and ETP/P ratios (Figure 6), we found an important difference between them: the Q/P ratios showed high interannual variation, while the ETP/P ratios were similar during the observation period. For example, in the annual Q estimates, the coefficient of variation (CV) ranged from 18.1% for riparian deciduous forest to 36.2% for mixed forest. For the annual ETP estimates, the coefficient of variation (CV) was much lower, ranging from 6.2% for the canopy gap to 10.3% for the riparian deciduous forest. Furthermore, our results show a strong linear trend between annual and seasonal Q and P for all urban forests, with Spearman correlation coefficients (R) ranging from 0.861 for the mixed forest to 0.967 for the riparian pine forest. The amount of P is the most important determinant for the amount of Q fluxes and consequently for the Q/P ratio. In contrast, there was no linear correlation with P in the annual ETP estimates ($p > 0.126$). For ETP fluxes and the ETP/P ratio, the most important determinant is the amount of TRAN.

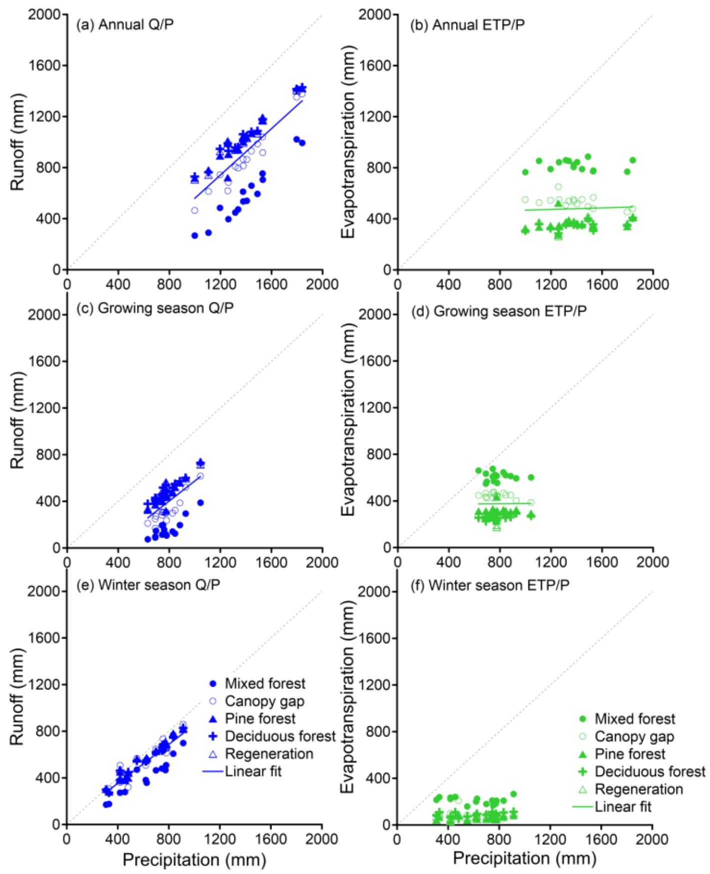

Figure 6. Relationship between (**a**) mean annual runoff–precipitation (Q/P) ratio, (**b**) mean annual evapotranspiration–precipitation (ETP/P) ratio, (**c**) mean growing season runoff–precipitation ratio (growing season Q/P), (**d**) mean growing season evapotranspiration–precipitation ratio (growing season ETP/P), (**e**) mean winter season runoff–precipitation ratio (winter season Q/P) and (**f**) mean winter season evapotranspiration–precipitation ratio (winter season ETP/P) for urban forests from 2007 to 2022.

4. Discussion

Understanding the water regulation ES of urban forests is an important goal of hydrologically orientated urban forest management, as well as urban water resources management and urban planning. Understanding the effects of urban forest structure and soil properties on water regulation ES is crucial for effective urban forest management to maintain the provision of hydrological ES [29] and mitigate the effects of natural water-related hazards [44]. Furthermore, the results of this study could help to promote urban forests as one of the urban "Natural Water Retention Measures" (NWRM) [42,43] and "Nature-Based Solutions" (NBS), as traditional approaches to urban water management (grey infrastructure) are often insufficient and unsustainable to mitigate the current and future impacts of climate change in urban areas [81–83].

The variables that influence hydrological fluxes and water regulation ES in a forest ecosystem are numerous and complex, arising from individual forest stand characteristics [24,25,84], soil properties [71,85], ecoregion [86], precipitation intensity [87,88] and seasonality [66,89]. Each forest ecosystem, defined by its stand structure, small-scale topography and soils, is to some extent unique. Therefore, it is difficult to draw general conclusions about water regulation ES by studying specific forest types and climatic zones.

The results of this study show that the provision of water regulation ES in selected urban forests is strongly influenced by stand structure (e.g., species composition, canopy and understorey geometry, age structure of forest stands, etc.) and soil properties. The optimal stand structure for maximum provision of water regulation ES, regardless of the season, was in the mixed forest, which, compared to the other urban forest types studied, is characterised by a significant proportion of evergreen conifers (especially the dominant spruce), a dense canopy, the highest growing stock, the deepest soils and the highest water-holding capacity of the soil.

4.1. Hydrological Fluxes in Urban Forests

One of the most important factors in the assessment and determination of hydrological fluxes is precipitation, which can refer to individual rainfall events or to a time interval in which several rainfall events have occurred [32]. As precipitation increases, the initial losses and infiltration capacity are met, resulting in Q. In addition to precipitation characteristics such as intensity, duration and distribution, certain physical aspects of watersheds influence the occurrence and quantity of runoff, such as soil type, vegetation, slope, contributing area and permeability [90]. Soil thickness and its spatial variation determine the geomorphology of slopes or watersheds and the associated water storage capacity, which in turn affects the hydraulic gradient, water movement and flow paths and thus controls the runoff processes [59].

Our study has shown that the structure of urban forests has a significant influence on water regulation ES. In addition, the variation of soil properties also had an important influence on the water regulation capacity of the urban forests studied. The simulated SMC ranged from 47 mm day^{-1} in the riparian regeneration to 292 mm day^{-1} in the canopy gap in the mixed (upland) forest, followed by the mixed forest (204 mm day^{-1}). These differences in SMC values are mainly due to soil properties, e.g., soil depth, stone content, texture, bulk density, etc. [71]. The SMC values were consistent with those reported by Meusburger et al. [71] for the Swiss forest, which ranged from 53 mm to 341 mm with a mean potential rooting depth of 1.2 m. Both plots in the mixed (upland) forest with the highest soil water-holding capacity have mineral soils classified as *Dystric Cambisols*, reaching up to 81 cm depth. In the canopy gap, almost all precipitation falls directly on the ground vegetation or soil, which has a smaller interception area than the multi-layered foliage of the forest stand [25]. In addition, the vegetation in the gaps has a lower water consumption compared to forests [91,92]. In contrast, the soil water-holding capacity was much lower in the riparian forests with shallower *Fluvisols* and up to 34% of the stone volume. The average daily SMC during the growing season was higher in the riparian deciduous forest (75 mm day^{-1}) than in the riparian regeneration (37 mm day^{-1}). In the riparian regeneration, the progressive growth of natural tree regeneration and edge trees led to increased canopy interception and increased root water extraction, resulting in lower SMC compared to the riparian pine and deciduous forests. Lower root density in belowground gaps reduces water uptake and transpiration via the roots [93]. For the beech-dominated Danish forest, it was found that the development of ground vegetation and regeneration can alter the gap effect as early as the second year after gap formation to reach forest conditions [94]. This is consistent with the results of our study, in which the progressive growth of natural tree regeneration and herbaceous vegetation in the riparian regeneration contributed to a similar annual ETP (27% of P) compared to riparian pine forest (26% of P) or the riparian deciduous forest (25% of P). The mixed forest had consistently higher annual ETP values (59% of P) than the riparian deciduous forest and the riparian pine forest. This may be attributed to the denser canopy in the mixed forest, a substantial assemblage of evergreen conifers (46% in growing stock) with broader crowns, especially the dominant spruce, and the highest growing stock (Table 1).

These are all the stand structure attributes that contribute to higher canopy interception [25,95,96], higher transpiration rates [97,98] and lower soil evaporation [99]. The estimated annual ETP in the mixed forest (59% of P) was similar to the annual ETP of the eucalypt plantation in southern China (Leizhou Peninsula), which ranged from 50% to 71% of annual P [100]. Nakai et al. [101] reported a higher annual ETP for the Alaska spruce (*Picea mariana* (Mill.) forest (86% of P). Ouyang et al. [102] also found higher annual ETP for the deciduous *S. wallichii*, *A. mangium* and the conifers *C. lanceolata* in the hilly areas of southern China (96%, 94% and 80% of P, respectively). In a black locust plantation on the semi-arid loess plateau in China, the ETP values for the growing season ranged from 69% to 104% of P [103], which is consistent with the ETP estimates for the growing season in the mixed forest in our study (76% of P). SE in the black locust plantation accounted for most of the growing season ETP (45–69% at the monthly level), while TRAN was the smallest component of ETP (10–29%). Similarly, in the canopy gap in our study, the growing season SE accounted for 46% of ETP and the growing season TRAN accounted for 53% of ETP at the monthly level. In other urban forests in our study, TRAN accounted for most of the growing season ETP at the monthly level (70% of ETP in riparian regeneration, 71% of ETP in mixed forest, and 73% of ETP in riparian pine forest, respectively). Tree transpiration was also the major water flux in a semi-arid pine forest in the Yatir forest in southern Israel, accounting for 49% of ETP, while SE accounted for 39% of ETP and I for 12% of ETP [104]. An exception in our study was riparian deciduous forest, for which I was an important component (40% of ETP at the monthly level) along with TRAN (57% of ETP). A high I value in the tree canopy is often associated with a high leaf area index [105], which is closely related to the canopy cover. The study by Livesley et al. [22] showed that urban street trees with a denser canopy (larger plant area index) intercepted more annual precipitation (44%) than street trees with a less dense canopy (29%). Birches and pines in a car park in the city of Ljubljana, Slovenia, intercepted 23% and 45% of P, respectively [19]. In streets, parks and natural forests on the North Shore of British Columbia, 46% to 67% of P was intercepted by deciduous trees in summer, and 71% to 82% of P was intercepted by conifers in summer and winter [106]. However, Asadian and Weiler [28] point out that interception losses are twice as high for trees in urban environments as for trees in natural forests. Possible factors contributing to these differences are UHI (urban areas where temperatures are significantly higher than in surrounding areas), larger distances between trees (edge effect) and open-grown canopies. This is consistent with the study by Inkiläinen et al. [24], who determined an I fraction of 9–21% of P for an urban deciduous forest in North Carolina, USA. This is consistent with the annual I estimates in our study (1–16% of P).

In all urban forests studied, ETP was significantly higher in the leafed period than in the leafless period (Table 3, Figure 5), which can be attributed to the seasonal variation of tree crowns [87]. Deciduous trees shed their leaves in winter, which contributes to a lower canopy interception in winter than in the growing season [25,107]. In contrast, the presence of foliage (in deciduous trees) during the leafed period is expected to increase the amount of precipitation intercepted in the canopy as well as transpiration values. The TRAN in the growing season in the mixed forest (56% of P) was similar to that reported by Guillén et al. [108] for maples (53% of P), similar to that reported by Ouyang et al. [102] of 60% of P in the deciduous *S. wallichii* and *A. mangium* and higher than 10% of P in the oaks in the mixed temperate deciduous forests in West Virginia, USA [108].

In the canopy gap, lower ETP compared to mature mixed forest tends to increase Q and contributes to lower water regulation capacity [72], as shown in our study. Accordingly, Q accounted for up to 62% of annual P in the canopy gap, indicating a lower water regulation capacity compared to mixed forest, for which the Brook90 model simulation showed that only 41% of annual P drained to the subsurface. Gap formation also increased water runoff in a mixed forest in Germany [91], in a silver fir-beech forest in the Dinaric Alps [109] and in a pure European beech forest in Denmark [94]. However, the progressive growth of natural tree regeneration and herbaceous vegetation in the riparian regeneration contributed to a similar annual Q (74% of annual P) compared to the riparian pine forest (74% of annual P) or the riparian deciduous forest (75% of annual P).

The mixed forest in our study had the highest water retention capacity because its spruce trees retained their foliage throughout the year and stored more winter precipitation than the leafless deciduous vegetation in the canopy gap, the riparian deciduous forest and the riparian regeneration. However, contrary to our expectations, the riparian pine forest had the lowest winter ETP of all urban forests in our study (7% of P). The riparian pine forest had the highest proportion of conifers (Scots pine at 79% in the growing stock), but had lower annual and seasonal I compared to mixed forest, riparian deciduous forest and riparian regeneration. In general, a higher proportion of deciduous trees in mixed forests contributes to higher throughfall and stemflow and lower I [25], especially due to the leafless winter season. However, at the time of our study, the riparian pine forest had a loose canopy, with the upper canopy of Scots pine being open and spacious. This forest also contained smaller deciduous tree species than the mixed forest (Table 1). Smaller canopies do not intercept as much precipitation as wider canopies. Xiao, McPherson, Simpson and Ustin [77] reported that the leafed period I for the mixed forest in Sacramento with a dense canopy dominated by large broadleaf evergreens and conifers was 36%, whereas I in an urban forest with a less dense canopy dominated by medium-sized conifers and deciduous trees was only 18%. This confirms that I in urban forests can be influenced by tree size within a forest stand, in addition to other characteristics.

4.2. Indicators of Water Regulation Ecosystem Services (ES)

The proposed indicators for urban forests water regulation ES, the runoff-precipitation (Q/P) and the evapotranspiration-precipitation (ETP/P) ratios, have been used on a global scale to assess the heat balance of the Earth's surface [58], to estimate seasonal ETP for large areas of mixed land cover using measured global eddy flux data [59], and to produce regional maps of ETP/P and Q/P ratios for the northeastern United States as part of the runoff mapping that was a necessary component of the acid deposition impact assessment [110]. At the regional scale, the annual partitioning of precipitation (P) into evapotranspiration (ETP) and water yield (Q) was used to assess forest water yield in response to climate warming using long-term experimental catchments across North America [111]. In addition, the competitive relationship between Q and ETP at a watershed scale was used to determine the vegetation threshold to prevent further decline in runoff in a semi-arid watershed in northern China [97].

Due to this broad applicability of ETP/P and Q/P ratios, we suggest using these ratios as an easy-to-use ES-based tool for urban watershed management [38] to improve hydrologically orientated urban forest management measures [40]. Furthermore, the ETP/P and Q/P ratios could also be used for optimised urban green infrastructure planning [41], as they can be assessed and compared for different urban ecosystems or green spaces [112,113].

According to the ETP/P and Q/P ratios in our study (Figure 4, Table 4), the lowest capacity for water regulation ES was found for the riparian deciduous forest with the highest annual Q/P (0.75) and the lowest ETP/P ratio (0.25). These results indicate that 75% of the annual P in this urban forest is discharged as runoff, and only 25% of the annual P was utilised by the vegetation or evaporated into the atmosphere as part of evapotranspiration. This was followed by riparian regeneration with similar annual Q/P and ETP/P ratios (0.74 and 0.26). In contrast, the mixed forest showed the highest capacity for water regulation ES. The annual Q/P ratio for this urban forest was lowest (0.41) and the ETP/P ratio was highest (0.59), indicating that only 41% of annual P is discharged as runoff and 59% of annual P is utilised by vegetation or evaporates into the atmosphere as part of evapotranspiration. The same pattern was observed in winter and in the growing season, with the lowest Q/P and the highest ETP/P ratio for the mixed forest. The canopy gap in the mixed forest was approximately in the middle with an annual Q/P = 0.62 and ETP/P = 0.39. In the growing season, the canopy gap with the Q/P (0.40) and ETP/P (0.39) showed a higher capacity for water regulation than the riparian forests, where Q/P ranged from 0.60 to 0.63 and ETP/P from 0.33 to 0.39, but they were lower than in the mixed forest (Q/P = 0.21; ETP/P = 0.77). The Q/P ratios in our study are consistent with those reported by Church et al. [110] for selected large land resource areas in the northern United States from 1951 to 1984, which ranged from 0.49 to 0.68. The ETP/P ratios in our study are consistent with those reported by Liu et al. [59] for the energy-limited (PET < P) zones of the Pacific North West (PNW), ranging from 0.38 to 0.60 1964–2006, but lower than those in the water-limited zones (PET $\geq$ P) of the PNW, ranging from 0.65 to 0.82. In addition, ETP/P of broadleaf *S. wallichii* and *A. mangium* plantations in hilly lands of southern China were higher than in our study, exceeding 1.00 during most of the dry season [102]. Moreover, in a watershed in northeastern Inner Mongolia in Hulun Buir, China, ETP/P ranged from 1.30 to 1.60 and was significantly higher in the forests and lower in the grasslands, which is a consequence of the dense understory and litter layer that help reduce soil evaporation by retaining soil moisture in the forested watersheds [97]. McDonald [57] reports that the ETP/P ratio in the forested region of the Mogollon Plateau in the USA averages about 0.90 annually. In winter, this ratio drops to 0.85, but in summer it rises slightly to over 0.95, as almost half of the total annual precipitation that falls in summer is almost entirely consumed by evapotranspiration [57].

The annual and seasonal ETP/P ratios for selected urban forests show little interannual variation compared to Q/P. Moreover, a strong linear trend between Q and P for all urban forests analysed shows that P is the main factor determining the amount of Q fluxes and consequently the Q/P ratio. This was confirmed by Ye et al. [114], who reported that Q increases with P, especially when the precipitation event exceeds 50 mm and the sum of antecedent soil moisture and P exceeds 300 mm. Liu et al. [59] also found that P is the dominant factor controlling the geographical patterns of long-term trends in the annual Q/P ratio over the PNW, especially in the semi-arid regions. In contrast, the annual or seasonal ETP/P ratio showed no statistically significant correlation with P and exhibited relatively little interannual variation. The main cause of ETP differences was TRAN fluxes, which are strongly influenced by plant physiology and can be affected by abiotic environmental conditions, but also by mycorrhizal associations, plant diseases, atmospheric CO_2 concentrations and nutrient availability [104]. Stand-level transpiration and total evapotranspiration were reported to increase only slightly with P in a mature oak-hickory forest in North Carolina, USA, which was attributed to an increase in I [115]. Likens et al. [116] and Church et al. [110] also showed that ETP in northern forest ecosystems can remain remarkably constant over time despite large annual fluctuations in P and ambient temperatures.

Based on our results, we suggest that the ETP/P ratio better reflects the water regulation ES of urban forest vegetation and soils and therefore proves to be a better indicator of the water regulation ES of urban forests compared to Q/P. ETP can be easily calculated from the water balance equation (Equation (1)) using P and Q data obtained from runoff monitoring stations, precipitation monitoring stations [97,110,114] or estimates from modelling [59,69].

The future application of the ETP/P ratio will be to quantify the role of different urban green spaces in regulating runoff and thus the urban water balance in the city of Ljubljana, as well as in a broader range of cities and climate types. For example, urban green spaces in the urban area of Luohe in the North China Plain made a positive but limited contribution to runoff regulation, accounting for 10% of total runoff, with similar responses in future scenarios with a higher proportion of urban green spaces [112]. In addition, knowledge of the ETP/P ratio of different urban forests could be used to assess the sensitivity to climate warming and hydrological resilience of different urban forest types, which refers to the ability of an ecosystem to absorb change and maintain or rapidly restore hydrological function [117]. It has been shown that the hydrological resilience of different forest types in North America is highest in mixed conifer–deciduous forests with the highest elasticity and stable water yields, while it is lowest in alpine sites [111]. Furthermore, the ETP/P ratio of different urban forests could be used to estimate their potential to mitigate extreme heat through evapotranspiration and shading. It has been shown that the number of annual heat hours can be significantly reduced by different green spaces in the German city of Karlsruhe [113].

Furthermore, it would be good to apply other physically based models for a similar analysis. Although BROOK90 provides a good physical representation of the hydrological process, it also has some limitations. BROOK90 models vegetation as a single layer and ignores vertical complexity, which affects ETP accuracy in multi-layered forests. For example, the model does not account for ground vegetation, which leads to an underestimation of PET in forests with a dense ground vegetation layer [69], such as the riparian pine and deciduous forests in our study. Additionally, the model assumes that all leaves transpire, which leads to overestimates of ETP in deciduous forests in autumn and winter [70]. Furthermore, the SE is not constrained during frost days, leading to a potential overestimation in winter. As canopy parameters are assumed to be constant, the model does not account for vegetation growth or reductions in LAI caused by pests or drought, which affect SE predictions [70]. In addition, the energy of snowpack and evaporation from high tree canopies is overestimated, requiring arbitrary correction factors. Albedo is fixed and does not adjust for solar angle, canopy structure or snow age, which affects radiation calculations. The PET estimate is based on the vapor pressure deficit and net energy, with the net energy affected by vague albedo assumptions [70]. To summarise, the applicability of the model in different urban environments and under different climatic conditions requires further validation. To improve the generalisability of the results, we plan to perform a cross-validation of the model.

5. Conclusions

As the importance of the hydrological ES of urban ecosystems is increasingly recognised, there is a growing need for tools that can inform decision-makers about the provision of water regulation ES and the impact of natural resource management on these services. Urban forests as a form of "green infrastructure" are one of the most important providers of ES in urban areas. The most recognised benefits arising from their hydrological role are stormwater runoff reduction, stormwater retention, flood regulation and water quality protection.

We investigated how variations in urban forest stand structure (e.g., species composition, canopy and understorey geometry, forest stand age structure, etc.) and soil properties affecting soil water-holding capacity influence water regulation ES in five different urban forests in the city of Ljubljana, Slovenia. For this purpose, two indicators for the assessment of water regulation ES for urban forests were selected and their applicability was tested: the runoff to precipitation ratio (Q/P) and the evapotranspiration to precipitation ratio (ETP/P).

Both indicators, the ETP/P and Q/P ratios, showed that the lowest capacity for water regulation was in the riparian deciduous forest (Q/P = 0.75; ETP/P = 0.25) and the highest in the mixed (upland) forest (Q/P = 0.41; ETP/P = 0.59). The same pattern was observed in winter and in the growing season, with the Q/P ratio being lowest and the ETP/P ratio highest in the mixed forest. However, the Q/P ratio showed strong interannual variation and a strong linear correlation with annual and seasonal P, whereas the ETP/P ratio remained consistent over time despite large annual P fluctuations in the years of observation.

We conclude that the ETP/P ratio better reflects the water regulation ES of urban forest vegetation and soils and therefore proves to be a better indicator of the water regulation ES of urban forests compared to Q/P.

The optimal stand structure for maximum provision of water regulation ES, regardless of season, was found in the mixed forest, which, compared to other urban forest types studied, is characterised by a significant proportion of evergreen conifers (especially dominant spruce), a dense canopy, the highest growing stock, the deepest soils and the highest water-holding capacity of the soil.

In the outlook, we would like to suggest possible future directions on this topic:

- Including a wider range of cities and climate types to test the generalisability of the results presented in this study;
- Perform a cross-validation of the model;
- Perform a similar analysis for other physically based models;
- Develop specific urban forest management plans tailored to different forest types and urban hydrological characteristics.

Supplementary Materials: The following supporting information can be downloaded at https://www.mdpi.com/article/10.3390/land14040809/s1, Table S1: Values of selected parameters used in the Brook90 model simulations; Table S2: Linear regression (y = a + b*x) coefficients, linear correlation coefficient (r), index of agreement (D), root mean square error (RMSE), and sample size (n) describing the goodness-of-fit between Brook90 model simulated (y) and measured (x) daily values for the daily soil moisture contents (mm day−1) and monthly throughfall (mm month−1) for two calibration periods; Figure S1: Mean monthly air temperature (T), precipitation (P) and potential reference crop evapotranspiration to precipitation ratio (PET/P) during growing season at Ljubljana meteorological station from 1981 to 2010 (first column) and from 2007 to 2022; Figure S2: Monthly throughfall (mm)—measured values and simulated with the Brook90 model for (a) the mixed (upland) forest; (b) forest canopy; (c) riparian pine forest; (d) riparian deciduous forest and (e) riparian forest regeneration from 2007 to 2022; Figure S3: Daily soil moisture contents (SMC, mm)—measured values and simulated with the Brook90 model for (a) the mixed (upland) forest; (b) forest canopy gap; (c) riparian pine forest; (d) riparian deciduous forest and (e) riparian forest regeneration from 2007 to 2022; Figure S4: Linear regression (y = a + b*x) and r coefficient describing the goodness-of-fit between Brook90 model simulated (y) and measured (x) daily values for the daily soil moisture content (SMC; mm day^{-1}) and monthly throughfall (TF; mm month^{-1}) for two calibration periods.

Funding: This research was funded by the Life+ EMoNFUr project—Establishing a monitoring network to assess lowland forest and urban plantation in Lombardy and urban forest in Slovenia (LIFE10 ENV/IT/000399), the Austrian Science Fund (FWF) I 6254-N, the Slovenian Research Agency within the project "Evaluation of the impact of rainfall interception on soil erosion" (J2-4489) and the core funding for the Program Group "Forest biology, ecology and technology" (P4–0107) and the Ministry of Agriculture, Forestry and Food of the Republic of Slovenia within the Public Forest Service Task 1/2.3 "Hydrological and protective forest functions".

Data Availability Statement: Data are contained within the article and Supplementary Materials. Further inquiries can be directed to the corresponding author.

Acknowledgments: We would like to thank many technical assistants and employees from the Slovenian Forestry Institute: Tina Brišnik, Samo Grbec, Iztok Sinjur, Andrej Verlič, Daniel Žlindra, Janez Kermavnar, Erika Kozamernik for creating Figure 1, etc. We also thank Mojca Šraj and Klavdija Lebar for collecting and sharing soil moisture data and Mateja Ribnikar from the Faculty of Civil Engineering at the University of Ljubljana for preparing the modeling data. We thank the anonymous reviewers for their helpful comments on the manuscript.

Conflicts of Interest: The author declares no conflicts of interest. The funders had no role in the design of the study; in the collection, analyses, or interpretation of data; in the writing of the manuscript; or in the decision to publish the results.

References

1. Costanza, R.; d'Arge, R.; de Groot, R.; Farber, S.; Grasso, M.; Hannon, B.; Limburg, K.; Naeem, S.; O'Neill, R.V.; Paruelo, J.; et al. The value of the world's ecosystem services and natural capital. *Nature* **1997**, *387*, 253–260. [CrossRef]
2. MEA. *Ecosystems and Human Well-Being: Synthesis*; MEA: Washington, DC, USA, 2005; p. 281.
3. de Groot, R.S.; Alkemade, R.; Braat, L.; Hein, L.; Willemen, L. Challenges in integrating the concept of ecosystem services and values in landscape planning, management and decision making. *Ecol. Complex.* **2010**, *7*, 260–272. [CrossRef]
4. Brauman, K.A.; Daily, G.C.; Duarte, T.K.e.; Mooney, H.A. The Nature and Value of Ecosystem Services: An Overview Highlighting Hydrologic Services. *Annu. Rev. Environ. Resour.* **2007**, *32*, 67–98. [CrossRef]
5. Wallace, K.J. Classification of ecosystem services: Problems and solutions. *Biol. Conserv.* **2007**, *139*, 235–246. [CrossRef]
6. Keeler, B.L.; Polasky, S.; Brauman, K.A.; Johnson, K.A.; Finlay, J.C.; O'Neill, A.; Kovacs, K.; Dalzell, B. Linking water quality and well-being for improved assessment and valuation of ecosystem services. *Proc. Natl. Acad. Sci. USA* **2012**, *109*, 18619–18624. [CrossRef] [PubMed]
7. Nedkov, S.; Campagne, S.; Borisova, B.; Krpec, P.; Prodanova, H.; Kokkoris, I.P.; Hristova, D.; Le Clec'h, S.; Santos-Martin, F.; Burkhard, B.; et al. Modeling water regulation ecosystem services: A review in the context of ecosystem accounting. *Ecosyst. Serv.* **2022**, *56*, 101458. [CrossRef]
8. Sun, G.; Hallema, D.; Asbjornsen, H. Ecohydrological processes and ecosystem services in the Anthropocene: A review. *Ecol. Process.* **2017**, *6*, 35. [CrossRef]
9. Vörösmarty, C.J. Global water assessment and potential contributions from Earth Systems Science. *Aquat. Sci.* **2002**, *64*, 328–351. [CrossRef]
10. Vose, J.M.; Sun, G.; Ford, C.R.; Bredemeier, M.; Otsuki, K.; Wei, X.; Zhang, Z.; Zhang, L. Forest ecohydrological research in the 21st century: What are the critical needs? *Ecohydrology* **2011**, *4*, 146–158. [CrossRef]
11. Dobbs, C.; Hernández-Moreno, Á.; Reyes-Paecke, S.; Miranda, M.D. Exploring temporal dynamics of urban ecosystem services in Latin America: The case of Bogota (Colombia) and Santiago (Chile). *Ecol. Indic.* **2018**, *85*, 1068–1080. [CrossRef]
12. Du, J.; Shi, C.-x. Effects of climatic factors and human activities on runoff of the Weihe River in recent decades. *Quat. Int.* **2012**, *282*, 58–65. [CrossRef]
13. Norman, L.M.; Villarreal, M.L.; Niraula, R.; Haberstich, M.; Wilson, N.R. Modelling Development of Riparian Ranchlands Using Ecosystem Services at the Aravaipa Watershed, SE Arizona. *Land* **2019**, *8*, 64. [CrossRef]
14. Zhang, B.; Xie, G.-d.; Li, N.; Wang, S. Effect of urban green space changes on the role of rainwater runoff reduction in Beijing, China. *Landscape Urban Plann.* **2015**, *140*, 8–16. [CrossRef]
15. Gong, Y.; Geng, X.; Wang, P.; Hu, S.; Wang, X. Impact of Urbanization-Driven Land Use Changes on Runoff in the Upstream Mountainous Basin of Baiyangdian, China: A Multi-Scenario Simulation Study. *Land* **2024**, *13*, 1374. [CrossRef]
16. Vigerstol, K.L.; Aukema, J.E. A comparison of tools for modeling freshwater ecosystem services. *J. Environ. Manag.* **2011**, *92*, 2403–2409. [CrossRef] [PubMed]
17. Bolund, P.; Hunhammar, S. Ecosystem services in urban areas. *Ecol. Econ.* **1999**, *29*, 293–301. [CrossRef]
18. Dobbs, C.; Kendal, D.; Nitschke, C.R. Multiple ecosystem services and disservices of the urban forest establishing their connections with landscape structure and sociodemographics. *Ecol. Indic.* **2014**, *43*, 44–55. [CrossRef]
19. Zabret, K.; Šraj, M. Rainfall Interception by Urban Trees and Their Impact on Potential Surface Runoff. *CLEAN Soil Air Water* **2019**, *47*, 1800327. [CrossRef]
20. Barth, N.-C.; Döll, P. Assessing the ecosystem service flood protection of a riparian forest by applying a cascade approach. *Ecosyst. Serv.* **2016**, *21*, 39–52. [CrossRef]
21. Paul, M.J.; Meyer, J.L. Streams in the Urban Landscape. *Annu. Rev. Ecol. Evol. System.* **2001**, *32*, 333–365. [CrossRef]
22. Livesley, S.J.; Baudinette, B.; Glover, D. Rainfall interception and stem flow by eucalypt street trees—The impacts of canopy density and bark type. *Urban For. Urban Green.* **2014**, *13*, 192–197. [CrossRef]
23. Ponte, S.; Oishi, A.C.; Sonti, N.F.; Locke, D.H.; Phillips, T.H.; Pavao-Zuckerman, M.A. Interactions between management context and tree water use influence stormwater management potential of urban forests. *Urban For. Urban Green.* **2024**, *95*, 128321. [CrossRef]

24. Inkiläinen, E.N.M.; McHale, M.R.; Blank, G.B.; James, A.L.; Nikinmaa, E. The role of the residential urban forest in regulating throughfall: A case study in Raleigh, North Carolina, USA. *Landscape Urban Plann.* **2013**, *119*, 91–103. [CrossRef]
25. Kermavnar, J.; Vilhar, U. Canopy precipitation interception in urban forests in relation to stand structure. *Urban Ecosyst.* **2017**, *20*, 1373–1387. [CrossRef]
26. Nytch, C.J.; Meléndez-Ackerman, E.J.; Pérez, M.-E.; Ortiz-Zayas, J.R. Rainfall interception by six urban trees in San Juan, Puerto Rico. *Urban Ecosyst.* **2019**, *22*, 103–115. [CrossRef]
27. Xiao, Q.; McPherson, E.G. Rainfall interception by Santa Monica's municipal urban forest. *Urban Ecosyst.* **2002**, *6*, 291–302. [CrossRef]
28. Asadian, Y.; Weiler, M. A New Approach in Measuring Rainfall Interception by Urban Trees in Coastal British Columbia. *Water Qual. Res. J. Can.* **2009**, *1*, 16–25.
29. Amini Parsa, V.; Istanbuly, M.N.; Kronenberg, J.; Russo, A.; Jabbarian Amiri, B. Urban Trees and Hydrological Ecosystem Service: A Novel Approach to Analyzing the Relationship Between Landscape Structure and Runoff Reduction. *Environ. Manag.* **2023**, *73*, 243–258. [CrossRef]
30. Jin, M.; Shepherd, J.M. Inclusion of Urban Landscape in a Climate Model: How Can Satellite Data Help? *Bull. Am. Meteorol. Soc.* **2005**, *86*, 681–690. [CrossRef]
31. Trusilova, K.; Jung, M.; Churkina, G.; Karstens, U.; Heimann, M.; Claussen, M. Urbanization Impacts on the Climate in Europe: Numerical Experiments by the PSU–NCAR Mesoscale Model (MM5). *J. Appl. Meteorol. Clim.* **2008**, *47*, 1442–1455. [CrossRef]
32. Machado, R.E.; Cardoso, T.O.; Mortene, M.H. Determination of runoff coefficient (C) in catchments based on analysis of precipitation and flow events. *Int. Soil Water Conserv. Res.* **2022**, *10*, 208–216. [CrossRef]
33. McGrane, S.J. Impacts of urbanisation on hydrological and water quality dynamics, and urban water management: A review. *Hydrol. Sci. J.* **2016**, *61*, 2295–2311. [CrossRef]
34. Wu, D.; Zheng, L.; Wang, Y.; Gong, J.; Li, J.; Chen, Q. Dynamics in construction land patterns and its impact on water-related ecosystem services in Chengdu-Chongqing urban agglomeration, China: A multi-scale study. *J. Clean. Prod.* **2024**, *469*, 143022. [CrossRef]
35. Zabret, K.; Rakovec, J.; Šraj, M. Influence of meteorological variables on rainfall partitioning for deciduous and coniferous tree species in urban area. *J. Hydrol.* **2018**, *558*, 29–41. [CrossRef]
36. Vilhar, U. The Urban Forest. Water Regulation and Purification. In *The Urban Forest. Cultivating Green Infrastructure for People and the Environment*; Pearlmutter, D., Calfapietra, C., Samson, R., O'Brien, L., Krajter Ostoić, S., Sanesi, G., Alonso del Amo, R., Eds.; Springer: Berlin/Heidelberg, Germany, 2017; pp. 41–47.
37. O'Driscoll, M.; Clinton, S.; Jefferson, A.; Manda, A.; McMillan, S. Urbanization effects on watershed hydrology and in-stream processes in the southern United States. *Water* **2010**, *2*, 605–648. [CrossRef]
38. Beck, S.M.; McHale, M.R.; Hess, G.R. Beyond Impervious: Urban Land-Cover Pattern Variation and Implications for Watershed Management. *Environ. Manag.* **2016**, *58*, 15–30. [CrossRef] [PubMed]
39. Hutt-Taylor, K.; Ziter, C.D. Private trees contribute uniquely to urban forest diversity, structure and service-based traits. *Urban. For. Urban Green.* **2022**, *78*, 127760. [CrossRef]
40. Schüler, G. Identification of flood-generating forest areas and forestry measures for water retention. *For. Snow Landsc. Res.* **2006**, *80*, 99–114.
41. Semeraro, T.; Scarano, A.; Buccolieri, R.; Santino, A.; Aarrevaara, E. Planning of Urban Green Spaces: An Ecological Perspective on Human Benefits. *Land* **2021**, *10*, 105. [CrossRef]
42. OIEAU. Natural Water Retention Measures. Available online: https://www.nwrm.eu/sites/default/files/documents-docs/53-nwrm-illustrated.pdf/ (accessed on 20 January 2025).
43. EEA. Water-Retention Potential of Europe's Forests. A European overview to Support Natural Water-Retention Measures. Available online: https://www.eea.europa.eu/en/analysis/publications/water-retention-potential-of-forests (accessed on 20 January 2025).
44. Stefanakis, A.I.; Calheiros, C.S.C.; Nikolaou, I. Nature-Based Solutions as a Tool in the New Circular Economic Model for Climate Change Adaptation. *Circ. Econ. Sustain.* **2021**, *1*, 303–318. [CrossRef]
45. Loose, A.; Jazbinšek Sršen, N.; Jankovič, M. *Ready for Tomorrow. The Ljubljana Environmental Protection Program to 2013*; City of Ljubljana, Department of Environmental Protection: Ljubljana, Slovenia, 2010; p. 18.
46. Zupančič, B. *Klimatografija Slovenije. Količina Padavin: Obdobje 1961–1990*; Hidrometeorološki Zavod Republike Slovenije: Ljubljana, Slovenia, 1995; p. 366.
47. Cools, N.; De Vos, B. Part X: Sampling and Analysis of Soil. Version 2020-1. In *Manual on Methods and Criteria for Harmonized Sampling, Assessment, Monitoring and Analysis of the effects of Air Pollution on Forests*; United Nations Economic Commission for Europe Convention on Long-range Transboundary Air Pollution, ICP Forests Programme Co-ordinating Centre, Thünen Institute of Forest Ecosystems: Eberswalde, Germany, 2020; p. 29.

48. Dobbertin, M.; Neumann, M.; Levanič, T.; Sanders, T.G.M.; Skudnik, M.; Krüger, I. Part V: Tree Growth Level II. Version 2020-1. In *Manual on Methods and Criteria for Harmonized Sampling, Assessment, Monitoring and Analysis of the Effects of Air Pollution on Forests*; United Nations Economic Commission for Europe Convention on Long-range Transboundary Air Pollution, ICP Forests Programme Co-ordinating Centre, Thünen Institute of Forest Ecosystems: Eberswalde, Germany, 2020; p. 19.
49. Vilhar, U.; Čarni, A.; Božič, G. Growth and vegetation characteristics of European black poplar (*Populus nigra* L.) in a floodplain forest along river Sava and temperature differencies among selected sites. *Folia Biol. Geol.* **2013**, *45*, 193–214.
50. Verlič, A.; Eler, K.; Ferlan, M.; Flajšman, K.; de Groot, M.; Hauptman, T.; Jurc, D.; Kobal, M.; Kutnar, L.; Levanič, T.; et al. *EMoNFUr–Establishing a Monitoring network To Assess Lowland Forest and Urban Plantation in Lombardy and Urban Forest in Slovenia: Final Project Report*; Gozdarski Inštitut Slovenije, Slovenian Forestry Institute: Ljubljana, Slovenia, 2014; p. 156.
51. WRB. *World Reference Base for Soil Resources 2006, First Update 2007*; IUSS, ISRIC, FAO: Rome, Italy, 2007; p. 115.
52. Guo, Z.; Xiao, X.; Li, D. An Assessment of Ecosystem Services: Water Flow Regulation and Hydroelectric Power Production. *Ecol. Appl.* **2000**, *10*, 925–936. [CrossRef]
53. Guo, Z.; Gan, Y. Ecosystem function for water retention and forest ecosystem conservation in a watershed of the Yangtze River. *Biodivers. Conserv.* **2002**, *11*, 599–614. [CrossRef]
54. Aghakouchak, A.; Habib, E. Application of a Conceptual Hydrologic Model in Teaching Hydrologic Processes. *Int. J. Eng. Educ.* **2010**, *26*, 963–973.
55. Staudt, K.; Serafimovich, A.; Siebicke, L.; Pyles, R.D.; Falge, E. Vertical structure of evapotranspiration at a forest site (a case study). *Agric. For. Meteorol.* **2011**, *151*, 709–729. [CrossRef]
56. Federer, C.A. *BROOK90 Manual: A Simulation Model for Evaporation, Soil Water and Streamflow*, version 3.1; USDA Forest Service: Durham, NH, USA, 1995; p. 40.
57. McDonald, J.E. On the Ratio of Evaporation to Precipitation. *Bull. Am. Meteorol. Soc.* **1961**, *42*, 185–189. [CrossRef]
58. Budyko, M.I. The heat balance of the Earth's surface. *Sov. Geogr.* **1961**, *2*, 3–13. [CrossRef]
59. Liu, M.; Adam, J.C.; Hamlet, A.F. Spatial-temporal variations of evapotranspiration and runoff/precipitation ratios responding to the changing climate in the Pacific Northwest during 1921–2006. *J. Geophys. Res. Atmos.* **2013**, *118*, 380–394. [CrossRef]
60. Allen, R.G.; Pereira, L.S.; Raes, D.; Smith, M. *Crop Evapotranspiration. Guidelines for Computing Crop Water Requirements*; FAO: Rome, Italy, 1998; p. 300.
61. Vilhar, U.; Žlindra, D. *30 Years of Forest Monitoring in Slovenia*, 2nd ed.; Založba Silva Slovenica, Gozdarski Inštitut Slovenije: Ljubljana, Slovenia, 2017; Volume 156, p. 64.
62. Ferretti, M.; Fischer, R. *Forest Monitoring. Terrestrial Methods in Europe with Outlook to North America and Asia*, 1st ed.; Elsevier: Amsterdam, The Netherlands, 2013; Volume 12, p. 507.
63. Sinjur, I.; Ferlan, M.; Simončič, P.; Vilhar, U. The Meteorological Stations Net of the Forestry Institute of Slovenia. *Gozdarski Vestnik* **2010**, *68*, 41–46.
64. Ribnikar, M. *Use of Brook90 Model for Estimation of Water Balance in Urban Forests*; Univerza v Ljubljani: Ljubljana, Slovenia, 2018.
65. Clarke, N.; Žlindra, D.; Ulrich, E.; Mosello, R.; Derome, J.; Derome, K.; König, N.; Lövblad, G.; Geppert, F.; Draaijers, G.P.J.; et al. Part XIV: Sampling and Analysis of Deposition. Version 2022-1. In *Manual on Methods and Criteria for Harmonized Sampling, Assessment, Monitoring and Analysis of the Effects of Air Pollution on Forests, Eds.), Part XIV, United Nations Economic Commission for Europe Convention on Long-range Transboundary Air Pollution*; ICP Forests Programme Co-ordinating Centre, Thünen Institute of Forest Ecosystems: Eberswalde, Germany, 2022; p. 34.
66. Siegert, C.M.; Levia, D.F.; Hudson, S.A.; Dowtin, A.L.; Zhang, F.; Mitchell, M.J. Small-scale topographic variability influences tree species distribution and canopy throughfall partitioning in a temperate deciduous forest. *For. Ecol. Manag.* **2016**, *359*, 109–117. [CrossRef]
67. Kermavnar, J. Stand Precipitation in Selected Urban Forests in the City of Ljubljana. Master's Thesis, Univerza v Ljubljani, Ljubljana, Slovenia, 2015.
68. Dirksen, C. *Soil Physics Measurements*; Catena Verl.: Reiskirchen, Germany, 1999; p. 154.
69. Vilhar, U.; Starr, M.; Katzensteiner, K.; Simončič, P.; Kajfež-Bogataj, L.; Diaci, J. Modelling drainage fluxes in managed and natural forests in the Dinaric karst: A model comparison study. *Eur. J. For. Res.* **2010**, *129*, 729–740. [CrossRef]
70. Vorobevskii, I.; Luong, T.T.; Kronenberg, R.; Grünwald, T.; Bernhofer, C. Modelling evaporation with local, regional and global BROOK90 frameworks: Importance of parameterization and forcing. *Hydrol. Earth Syst. Sci.* **2022**, *26*, 3177–3239. [CrossRef]
71. Meusburger, K.; Trotsiuk, V.; Schmidt-Walter, P.; Baltensweiler, A.; Brun, P.; Bernhard, F.; Gharun, M.; Habel, R.; Hagedorn, F.; Köchli, R.; et al. Soil–plant interactions modulated water availability of Swiss forests during the 2015 and 2018 droughts. *Glob. Change Biol.* **2022**, *28*, 5928–5944. [CrossRef] [PubMed]
72. Vilhar, U. Water Regulation Ecosystem Services Following Gap Formation in Fir-Beech Forests in the Dinaric Karst. *Forests* **2021**, *12*, 224. [CrossRef]
73. Shuttleworth, W.J.; Wallace, J.S. Evaporation from sparse crops-an energy combination theory. *Quart. J. Royal Meteorol. Soc.* **1985**, *111*, 839–855. [CrossRef]

74. Federer, C.A.; Vorosmarthy, C.; Fekete, B. Sensitivity of Annual Evaporation to Soil and Root Properties in Two Models of Contrasting Complexity. *J. Hydrometeorol.* **2003**, *4*, 1276–1290. [CrossRef]
75. Thompson, S.A. *Hydrology for Water Management*; Balkema: Rotterdam, The Netherlands, 1999; p. 476.
76. *GraphPad Prism 10*; Version 10.4.0 (621); GraphPad Software, LLC.; Dotmatics: Boston, MA, USA, 2024.
77. Xiao, Q.F.; McPherson, E.G.; Simpson, J.R.; Ustin, S.L. Rainfall interception by Sacramento's urban forest. *J. Arboric.* **1998**, *24*, 235–244. [CrossRef]
78. Aalbers, E.E.; van Meijgaard, E.; Lenderink, G.; de Vries, H.; van den Hurk, B.J.J.M. The 2018 west-central European drought projected in a warmer climate: How much drier can it get? *Nat. Hazards Earth Syst. Sci.* **2023**, *23*, 1921–1946. [CrossRef]
79. Gessner, C.; Fischer, E.M.; Beyerle, U.; Knutti, R. Multi-year drought storylines for Europe and North America from an iteratively perturbed global climate model. *Weather Clim. Extrem.* **2022**, *38*, 100512. [CrossRef]
80. Moravec, V.; Markonis, Y.; Rakovec, O.; Svoboda, M.; Trnka, M.; Kumar, R.; Hanel, M. Europe under multi-year droughts: How severe was the 2014–2018 drought period? *Environ. Res. Lett.* **2021**, *16*, 034062. [CrossRef]
81. Carlyle-Moses, D.E.; Livesley, S.J.; Baptista, M.D.; Thom, J.K.; Szota, C. Urban Trees as Green Infrastructure for Stormwater Mitigation and Use. *Ecol. Stud.* **2020**, *240*, 397–432.
82. Wang, J.; Endreny, T.A.; Nowak, D.J. Mechanistic Simulation of Tree Effects in an Urban Water Balance Model. *JAWRA J. Am. Water Resour. Assoc.* **2008**, *44*, 75–85. [CrossRef]
83. Hamel, P.; Tan, L. Blue–Green Infrastructure for Flood and Water Quality Management in Southeast Asia: Evidence and Knowledge Gaps. *Environ. Manag.* **2022**, *69*, 699–718. [CrossRef] [PubMed]
84. Li, X.; Xiao, Q.; Niu, J.; Dymond, S.; van Doorn, N.S.; Yu, X.; Xie, B.; Lv, X.; Zhang, K.; Li, J. Process-based rainfall interception by small trees in Northern China: The effect of rainfall traits and crown structure characteristics. *Agric. For. Meteorol.* **2016**, *218–219*, 65–73. [CrossRef]
85. Li, K.; Wang, G.; Gao, J.; Guo, L.; Li, J.; Guan, M. The rainfall threshold of forest cover for regulating extreme floods in mountainous catchments. *Catena* **2024**, *236*, 107707. [CrossRef]
86. Zimmermann, A.; Wilcke, W.; Elsenbeer, H. Spatial and temporal patterns of throughfall quantity and quality in a tropical montane forest in Ecuador. *J. Hydrol.* **2007**, *343*, 80–96. [CrossRef]
87. Bryant, M.L.; Bhat, S.; Jacobs, J.M. Measurements and modeling of throughfall variability for five forest communities in the southeastern US. *J. Hydrol.* **2005**, *312*, 95–108. [CrossRef]
88. Šraj, M.; Brilly, M.; Mikoš, M. Rainfall interception by two deciduous Mediterranean forests of contrasting stature in Slovenia. *Agric. For. Meteorol.* **2008**, *148*, 121–134. [CrossRef]
89. Deguchi, A.; Hattori, S.; Park, H.-T. The influence of seasonal changes in canopy structure on interception loss: Application of the revised Gash model. *J. Hydrol.* **2006**, *318*, 80–102. [CrossRef]
90. Wang, F.; Wang, G.; Cui, J.; Guo, L.; Tang, X.; Yang, R.; Du, J.; Sadegh Askari, M. The nonlinear rainfall–quick flow relationships in a humid mountainous area: Roles of soil thickness and forest types. *J. Hydrol.* **2024**, *648*, 131854. [CrossRef]
91. Zirlewagen, D.; von Wilpert, K. Modeling water and ion fluxes in a highly structured, mixed-species stand. *For. Ecol. Manag.* **2001**, *143*, 27–37. [CrossRef]
92. Cognard-Plancq, A.-L.; Marc, V.; Didon-Lescot, J.-F.; Norman, M. The role of forest cover on streamflow down sub-Mediterranean mountain watersheds: A modelling approach. *J. Hydrol.* **2001**, *254*, 229–243. [CrossRef]
93. Ritter, E.; Dalsgaard, L.; Einhorn, K.S. Light, temperature and soil moisture regimes following gap formation in a semi-natural beech-dominated forest in Denmark. *For. Ecol. Manag.* **2005**, *206*, 15–33. [CrossRef]
94. Ritter, E.; Starr, M.; Vesterdal, L. Losses of nitrate from gaps of different sizes in a managed beech (Fagus sylvatica) forest. *Can. J. For. Res.* **2005**, *35*, 308–319. [CrossRef]
95. Tobón Marin, C.; Bouten, W.; Sevink, J. Gross rainfall and its partitioning into throughfall, stemflow and evaporation of intercepted water in four forest ecosystems in western Amazonia. *J. Hydrol.* **2000**, *237*, 40–57. [CrossRef]
96. Cleophas, F.; Mahali, M.; Musta, B.; Zahari, N.Z.; Lee, L.E.; Bidin, K. Canopy precipitation interception in a lowland tropical forest in relation to stand structure. *IOP Conf. Ser. Earth Environ. Sci.* **2022**, *1053*, 012005. [CrossRef]
97. Fang, Q.; Xin, X.; Guan, T.; Wang, G.; Zhang, S.; Ma, M. Vegetation patterns governing the competitive relationship between runoff and evapotranspiration using a novel water balance model at a semi-arid watershed. *Environ. Res.* **2022**, *214*, 113976. [CrossRef]
98. Rötzer, T.; Häberle, K.H.; Kallenbach, C.; Matyssek, R.; Schütze, G.; Pretzsch, H. Tree species and size drive water consumption of beech/spruce forests—A simulation study highlighting growth under water limitation. *Plant Soil* **2017**, *418*, 337–356. [CrossRef]
99. Peng, L.; Zeng, Z.; Wei, Z.; Chen, A.; Wood, E.F.; Sheffield, J. Determinants of the ratio of actual to potential evapotranspiration. *Glob. Change Biol.* **2019**, *25*, 1326–1343. [CrossRef]
100. Lane, P.N.J.; Morris, J.; Ningnan, Z.; Guangyi, Z.; Guoyi, Z.; Daping, X. Water balance of tropical eucalypt plantations in south-eastern China. *Agric. For. Meteorol.* **2004**, *124*, 253–267. [CrossRef]

101. Nakai, T.; Kim, Y.; Busey, R.C.; Suzuki, R.; Nagai, S.; Kobayashi, H.; Park, H.; Sugiura, K.; Ito, A. Characteristics of evapotranspiration from a permafrost black spruce forest in interior Alaska. *Polar Sci.* **2013**, *7*, 136–148. [CrossRef]
102. Ouyang, L.; Wu, J.; Zhao, P.; Li, Y.; Zhu, L.; Ni, G.; Rao, X. Consumption of precipitation by evapotranspiration indicates potential drought for broadleaved and coniferous plantations in hilly lands of South China. *Agric. Water Manag.* **2021**, *252*, 106927. [CrossRef]
103. Jiao, L.; Lu, N.; Fu, B.; Wang, J.; Li, Z.; Fang, W.; Liu, J.; Wang, C.; Zhang, L. Evapotranspiration partitioning and its implications for plant water use strategy: Evidence from a black locust plantation in the semi-arid Loess Plateau, China. *For. Ecol. Manag.* **2018**, *424*, 428–438. [CrossRef]
104. Raz-Yaseef, N.; Yakir, D.; Schiller, G.; Cohen, S. Dynamics of evapotranspiration partitioning in a semi-arid forest as affected by temporal rainfall patterns. *Agric. For. Meteorol.* **2012**, *157*, 77–85. [CrossRef]
105. Nooraei Beidokhti, A.; Moore, T.L. The effects of precipitation, tree phenology, leaf area index, and bark characteristics on throughfall rates by urban trees: A meta-data analysis. *Urban For. Urban Green.* **2021**, *60*, 127052. [CrossRef]
106. Asadian, Y. Rainfall Interception in an Urban Environment. Master's Thesis, The University of British Columbia, Vancouver, BC, Canada, 2010.
107. Xiao, Q.; McPherson, E.G. Rainfall interception of three trees in Oakland, California. *Urban Ecosyst.* **2011**, *14*, 755–769. [CrossRef]
108. Guillén, L.A.; Brzostek, E.; McNeil, B.; Raczka, N.; Casey, B.; Zegre, N. Sap flow velocities of Acer saccharum and Quercus velutina during drought: Insights and implications from a throughfall exclusion experiment in West Virginia, USA. *Sci. Total Environ.* **2022**, *850*, 158029. [CrossRef]
109. Vilhar, U.; Simončič, P. Water status and drought stress after gap formation in managed and semi-natural silver fir-beech forests. *Eur. J. For. Res.* **2012**, *131*, 1381–1397. [CrossRef]
110. Church, M.R.; Bishop, G.D.; Cassell, D.L. Maps of regional evapotranspiration and runoff/precipitation ratios in the northeast United States. *J. Hydrol.* **1995**, *168*, 283–298. [CrossRef]
111. Creed, I.F.; Spargo, A.T.; Jones, J.A.; Buttle, J.M.; Adams, M.B.; Beall, F.D.; Booth, E.; Campbell, J.; Clow, D.; Elder, K.; et al. Changing forest water yields in response to climate warming: Results from long-term experimental watershed sites across North America. *Glob. Change Biol.* **2014**, *20*, 3191–3208. [CrossRef]
112. Song, P.; Guo, J.; Xu, E.; Mayer, A.L.; Liu, C.; Huang, J.; Tian, G.; Kim, G. Hydrological Effects of Urban Green Space on Stormwater Runoff Reduction in Luohe, China. *Sustainability* **2020**, *12*, 6599. [CrossRef]
113. Pace, R.; Endreny, T.A.; Ciolfi, M.; Gangwisch, M.; Saha, S.; Ruehr, N.K.; Grote, R. Mitigation potential of urban greening during heatwaves and stormwater events: A modeling study for Karlsruhe, Germany. *Sci. Rep.* **2025**, *15*, 5308. [CrossRef] [PubMed]
114. Ye, S.; Liu, L.; Li, J.; Pan, H.; Li, W.; Ran, Q. From rainfall to runoff: The role of soil moisture in a mountainous catchment. *J. Hydrol.* **2023**, *625*, 130060. [CrossRef]
115. Oishi, A.C.; Oren, R.; Novick, K.A.; Palmroth, S.; Katul, G.G. Interannual Invariability of Forest Evapotranspiration and Its Consequence to Water Flow Downstream. *Ecosystems* **2010**, *13*, 421–436. [CrossRef]
116. Likens, G.E.; Bormann, F.E.; Pierce, R.S.; Eaton, J.S.; Johnson, N.M. *Biogeochemistry of a Forested Ecosystem*; Springer: New York, NY, USA, 1977.
117. Gerten, D.; Lucht, W.; Schaphoff, S.; Cramer, W.; Hickler, T.; Wagner, W. Hydrologic resilience of the terrestrial biosphere. *Geophys. Res. Lett.* **2005**, *32*, L21408. [CrossRef]